Monthly Notices
of the
ROYAL ASTRONOMICAL SOCIETY

MNRAS **442,** 3065–3072 (2014) doi:10.1093/mnras/stu1054

A *Herschel* PACS survey of brown dwarfs in IC 2391: limits on primordial and debris disc fractions

B. Riaz[1]⋆ and G. M. Kennedy[2]

[1]*Centre for Astrophysics Research, Science & Technology Research Institute, University of Hertfordshire, Hatfield AL10 9AB, UK*
[2]*Institute of Astronomy, University of Cambridge, Madingley Road, Cambridge CB3 0HA, UK*

Accepted 2014 May 25. Received 2014 May 19; in original form 2014 February 27

ABSTRACT

We present results from a *Herschel* Photodetector Array Camera and Spectrometer (PACS) survey of eight brown dwarfs in the IC 2391 cluster. Our aim was to determine the brown dwarf disc fraction at ages of ∼40–50 Myr. None of the eight brown dwarfs observed were detected in the PACS 70 or 160 μm bands. We have determined the detection limits of our survey using the 1σ flux upper limits in the PACS far-infrared and the *Wide-field Infrared Survey Telescope* mid-infrared bands. The sensitivity of our observations would only allow for the detection of debris discs with exceptionally large fractional luminosities ($\geq$1 per cent). Considering that only the most extreme and rare debris discs have such high fractional luminosities, it can be hypothesized that Vega-like debris discs, as observed around ∼30 per cent of low-mass stars at similar ages, could exist around the targeted IC 2391 brown dwarfs. Most primordial discs similar to the ones observed for the younger 1–10 Myr brown dwarfs would be within the detection sensitivities of our survey, and could have been detected. The non-detection for all targets then suggests that brown dwarf discs have transitioned to the debris phase by ∼40–50 Myr ages. We also present the sensitivity limits for detecting brown dwarf discs with future *SPICA* observations.

Key words: brown dwarfs – circumstellar matter – stars: low-mass – open clusters and associations: individual: IC 2391.

1 INTRODUCTION

Low-mass pre-main-sequence stars are formed with substantial rotating discs around them. These optically thick primordial discs are massive and have an initial gas:dust ratio similar to the interstellar ratio. As the system evolves, the primordial disc gradually dissipates, resulting in a decrease in the total disc mass. The dissipation may occur through various processes. Much of the disc may be accreted on to the central star; some material may be driven off by stellar winds (e.g. Gullbring et al. 1998; Muzerolle et al. 1998; Calvet et al. 2005). The dissipation may also occur through the coagulation of the smaller particles to form larger planetesimals, which may eventually lead to planet formation (e.g. Rice et al. 2003; Dullemond & Dominik 2004; Quillen et al. 2004; Setiawan et al. 2008). The collisions among the planetesimals produce dust grains that form the secondary debris discs. These are gas-poor discs, comprised of dust which is continually regenerated as the larger and more massive planetesimals trigger shattering collisions amongst the smaller bodies. Dissipation in the debris discs occurs as the mass reservoir of large planetesimals, which supplies the observed dust, is depleted (e.g. Wyatt 2008), whereas the smallest (<1 μm) dust is removed by radiation and stellar wind forces (e.g. Burns et al. 1979; Plavchan et al. 2009).

Recent near- and mid-infrared surveys of clusters and associations spanning a range in ages and masses have revealed extensive information on the disc frequencies and lifetimes. The main finding from these surveys is that optically thick primordial discs are extensively dissipated by an age of ∼10 Myr (e.g. Strom et al. 1989; Haisch, Lada & Lada 2001; Young et al. 2004; Hillenbrand 2008). It is also at this critical age of ∼10 Myr that a rise in the debris disc frequency is observed. Debris discs are commonly detected at ∼10–30 Myr as they are bright and have not had much time to decay yet. Thereafter, the frequency declines roughly as 1/t over a time-scale of a few hundred Myr (e.g. Rieke et al. 2005; Siegler et al. 2007; Carpenter et al. 2009).

Also notable is the dependence of the decay time-scales on the spectral type of the central source. As discussed in Riaz et al. (2012), the primordial disc lifetime appears prolonged in very low mass stars and brown dwarfs compared to the higher mass stars, such that nearly all brown dwarf discs at an age of ∼10 Myr are in the primordial stage, compared to an ∼10 per cent fraction for low-mass stars (0.1–1 $M_\odot$) and a null fraction for >1 $M_\odot$ stars. For the debris discs, the inner disc decay time-scales, as probed

⋆ E-mail: b.riaz@herts.ac.uk

Table 1. Observations.

ID	Position (J2000)	ObsID	$T_{\rm eff}$	log L	SpT	3.4 μm[a] (err)	SNR	4.6 μm (err)	SNR	12 μm (err)	SNR	22 μm (err)	SNR	70 μm[b]	160 μm
1	083847.07-521456.4	1342265624/5	2800	−2.85	M6	14.00 (0.025)	43.7	13.726 (0.029)	37.6	12.479 (null)	−0.6	9.322 (null)	−1.3	0.93	5.26
2	083847.30-524432.7	1342265620/1	2800	−2.575	M6	13.864 (0.026)	41.6	13.589 (0.029)	37.7	13.176 (null)	−2.3	9.336 (null)	−2.1	1.54	17.38
3	084218.71-523940.1	1342265505/6	2575	−2.70	M7	13.569 (0.024)	44.6	13.408 (0.026)	41.3	12.638 (null)	−0.7	9.313 (null)	−0.5	0.92	7.44
4	084323.67-531416.9	1342265503/4	2800	−2.75	M6	13.762 (0.025)	42.9	13.690 (0.028)	39.3	12.259 (null)	0.6	9.095 (null)	0.2	0.89	6.66
5[c]	084402.10-524410.7	1342270971/2	2575	−2.70	M7	13.612 (0.034)	32.3	13.432 (0.035)	31.2	12.088 (0.22)	4.9	9.172 (null)	−0.6	1.15	14.72
6	083618.24-532557.6	1342270969/70	2654	−2.89	M7.5	14.059 (0.026)	41.1	13.831 (0.033)	33.2	12.966 (null)	−0.2	9.514 (null)	−1.9	0.85	3.46
7	083933.26-524710.4	1342265507/8	2958	−2.55	M6.5	13.639 (0.030)	35.6	13.416 (0.030)	36.0	12.372 (0.236)	4.6	8.962 (null)	1.1	1.15	7.38
8	084016.67-523658.3	1342265622/3	2740	−2.81	M6.5	14.616 (0.027)	40.8	14.424 (0.044)	24.5	12.790 (null)	−0.9	8.978 (null)	0.3	0.98	7.26

[a] *WISE* photometry. A 'null' error and a negative SNR imply a non-detection.
[b] PACS 70 and 160 μm 1σ flux upper limits in units of mJy.
[c] The photometry for the target ID #5 was found in the AllWISE Reject Table, because it is affected by a diffraction spike from a nearby star.

by 24 μm dust emission, appear shorter for the FGKM stars compared to the more massive B- and A-type stars (e.g. Beichman et al. 2006; Siegler et al. 2007). The rapid inside out evacuation of disc material suggests that processes such as planet formation are completed inside ∼1 au within 30–50 Myr for the low-mass stars, resulting in very few 24 μm disc detections at these later ages (e.g. Gorlova et al. 2007; Spezzi et al. 2009). Other processes such as, Poynting–Robertson drag, stellar wind drag, or planet–dust dynamical interactions may also be responsible for shortening the dust grain removal time-scales (e.g. Plavchan et al. 2009). It should be noted that 24 μm observations of nearby stars are more sensitive, which explains why a higher fraction (∼5 per cent; Trilling et al. 2008) of these stars are seen to have 24 μm excesses, compared to observations of young clusters such as IC 2391 and NGC 2547. On the other hand, the differences in the disc frequency trends could be due to a luminosity effect rather than a mass-dependent effect, as the more massive stars heat up dust at larger annuli to the levels detectable at mid- and far-infrared wavelengths. The low stellar luminosities could make even a 10 au disc so cold that it can only be detected at far-infrared wavelengths, as observed to be the case for the disc around Fomalhaut C, which is only detected at >100 μm wavelengths (Kennedy et al. 2014).

The search for debris discs around brown dwarfs is a field which has not been explored to great lengths yet. Previous surveys on brown dwarf discs based on mid- and far-infrared observations have all focused on ages of <10 Myr, at which brown dwarf discs are still found to be in the primordial phase (Riaz & Gizis 2008; Harvey et al. 2012; Riaz et al. 2012). We have conducted a photometric survey of brown dwarfs in the ∼40–50 Myr old cluster IC 2391, using the ESA *Herschel* Space Observatory (Pilbratt et al. 2010) Photodetector Array Camera and Spectrometer (PACS; Poglitsch et al. 2010) instrument (70 and 160 μm), to search for cold dust emission that would indicate the presence of debris discs. Considering the trends noted above, no clear transition from a primordial to a debris phase is observed for the brown dwarf discs even at ∼10 Myr ages, unlike the higher mass stars. Our main scientific goal is to map the evolution of brown dwarf discs over a wider age range, and to determine if the onset of the debris phase occurs at a later age for the sub-stellar sources, compared to the earlier-type stars.

2 OBSERVATIONS AND DATA ANALYSIS

We searched for nearby pre-main-sequence clusters with an estimated age of ∼30–50 Myr, and which contain spectroscopically confirmed sub-stellar members with masses below 0.08 $M_\odot$. At ∼30–50 Myr, this sub-stellar mass limit corresponds to a $T_{\rm eff}$ of less than ∼2900 K and a spectral type ≥M6 (e.g. Baraffe et al. 2003). The IC 2391 cluster is therefore of interest. It has an age of 50 Myr estimated via the lithium method (Barrado y Navacues et al. 2004) and 40 Myr from main-sequence fitting (Platais et al. 2007) and lies at a distance of 145 ± 2.5 pc (van Leeuwen 2007). There are currently about 10 spectroscopically confirmed brown dwarfs in this cluster with spectral type ≥M6 and masses below 0.07 $M_\odot$ (Barrado y Navacues et al. 2004; Boudreault et al. 2009). We obtained PACS 70 and 160 μm photometric observations under *Herschel* Cycle 2 (PID: OT2_briaz_4) for eight brown dwarfs in IC 2391 (Table 1). All observations were made using the mini-scan map mode. Two cross-scans were obtained at orientation angles of 77° and 110°, with a scan leg length of 2.5 arcmin, cross-scan step of 4 arcsec, and 10 scan legs for each scan. The medium scan speed (20 arcsec s^{-1}) was used as it provides optimum sensitivity. The 1σ rms noise level using six repeats of this setup was expected to be ∼1 mJy at 70 μm, using the HSPOT tool.

Data analysis was performed on the 'Level 2' data products processed using the *Herschel* Interactive Processing Environment (HIPE version 11.0.1). We created a mosaic of the two scan maps obtained at different orientation angles. The 160 μm images do not cover exactly the same sky area as the 70 μm images, even though these were observed simultaneously; one of the red band arrays expired in the last few months of *Herschel* operation, which is presumably the reason for the difference in the coverage area. None of the targets were detected in any of the PACS bands at the expected source location in the maps. The objects with ID #1 and 4 have a point source located about 10 arcsec away in each case (Fig. 1), but considering that the *Herschel* pointing was good to about 1 arcsec, these sources are unrelated to the targets in question. There is some scattered emission observed close to the target location for objects with ID #3, 6 and 8, which cannot be confirmed as a point-like source detection. We measured the 1σ noise in the maps by placing a large number of apertures at random locations in each map, and then taking the standard deviation of these measurements. The aperture sizes were set to 4 and 8 arcsec, which are the optimal signal-to-noise ratio (SNR) sizes at 70 and 160 μm. The 1σ noise levels thus derived are listed in Table 1. The noise measurements are not as similar to one another at 160 μm as expected given the same integration times. However, putting all the images together on the sky and comparing with the IRAS 100 μm levels (Fig. 2) seems to give sensible results when compared with the derived noise levels. The 160 μm noise is quite a bit higher than at 70 μm. This is in part due to instrument sensitivities, but is also related to the loss of some of the red array. Looking at the individual images, there is some background structure that will have also contributed (Fig. 2).

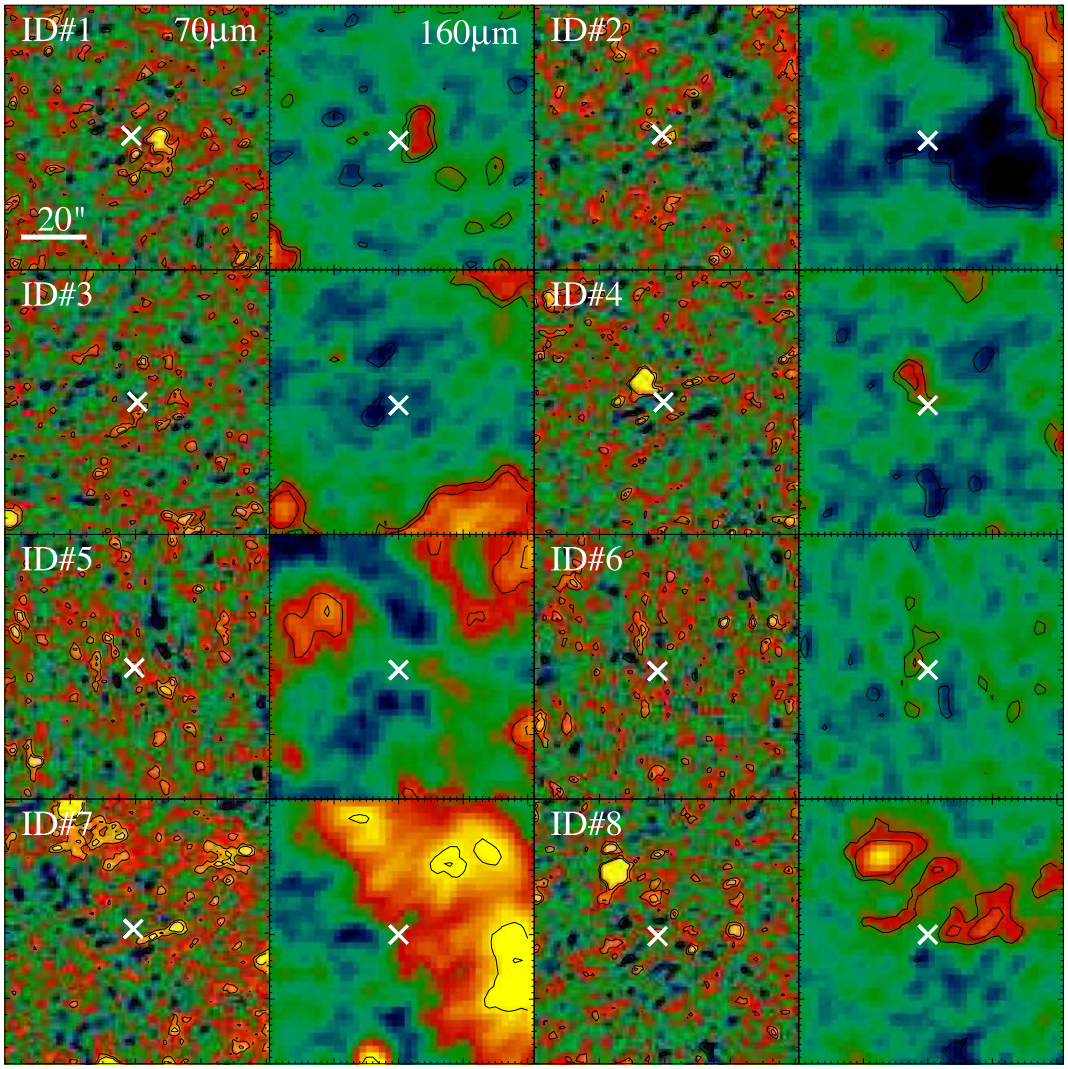

Figure 1. PACS 70 and 160 μm images for the eight targets. White crosses mark the target positions, which are close to the centre of each image. Each image is 80 arcsec^2, and the colour scale is a linear stretch from -5 to 8×10^{-5} Jy pixel^{-1} at 70 μm, and -4 to 8×10^{-4} Jy pixel^{-1} at 160 μm. Contours are shown at -3, -2, 2, and 3 times the pixel to pixel rms for each image. North is up, east is to the left.

The targets with ID #2, 5 and 7 lie along a brighter region and also have higher noise, whereas ID #6, 1 and 4 have the flattest looking maps and these have the lowest 160 μm noise. The 70 μm maps thus appear sky noise limited, while the 160 μm maps are background limited, with perhaps ID #6 being sky noise limited at 160 μm.

We also checked for matches in the *Wide-field Infrared Survey Telescope* (*WISE*; Wright et al. 2010) data base. We used the ALLWISE Source Catalog, which provides better sensitivities and depth-of-coverage than the *WISE* All-Sky Source Catalog. Out of the eight targets, seven objects have *WISE* counterparts within 10 arcsec of the target position, while one target (ID #5) is listed in the ALLWISE Reject Catalog due to contamination by a diffraction spike from a nearby source. All of the seven objects with *WISE* counterparts are detected in the 3.4 and 4.6 μm bands at an SNR > 20 (Table 1). None are convincingly detected in the 12 and 22 μm bands, as indicated by the low SNR and by checking the individual *WISE* images. We have considered the 12 and 22 μm photometry as upper limits for all sources. The spectral energy distributions (SEDs) for the targets combining all photometry are shown in Fig. 3. We have used the BT Settl models (Allard et al. 2003) to fit the photospheric emission. The normalization of the atmosphere fits is to the ($J-$[4.6]) photometry via least-squares fitting, with $T_{\rm eff}$ fixed. The filled circles and triangles are the observed photometry and upper limits, respectively. The upper limits in the *WISE* 12 and 22 μm bands and the PACS bands appear in excess to the photospheric emission for all targets.

3 RESULTS AND DISCUSSION

3.1 Fractional debris disc luminosities

The non-detection of cold debris dust could be due to the poor sensitivities of our survey. To probe further into how bright a debris disc around the targeted brown dwarfs would need to be in order to be detectable, we have converted the detection limits (or the 1σ upper limits) into the fractional disc luminosity, $L_{\rm disc}/L_*$, for each source, as shown in Fig. 4. The contours in the plot show how bright a disc with a specific temperature and fractional luminosity could have been detected around how many of the targeted brown dwarfs, given the upper limits obtained from the observations. We assume that the gaseous material has dispersed, therefore the fractional luminosities correspond to dust emission only. We assume

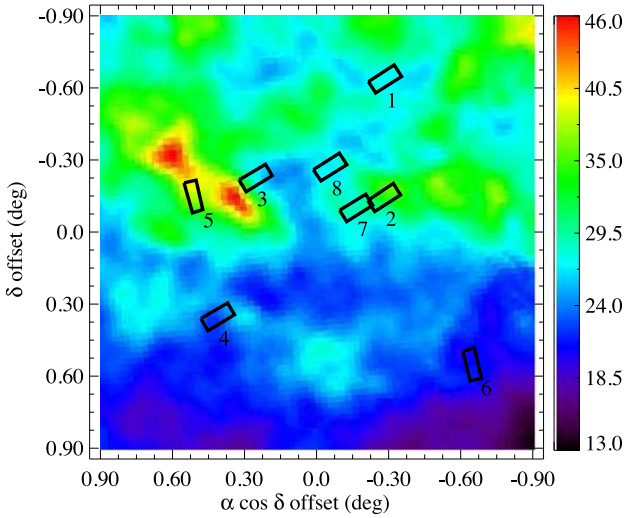

Figure 2. A comparison of the PACS image locations with the IRAS 100 μm noise levels (Miville-Deschenes & Lagache 2005). The scale on the right is in MJy sr^{-1}. The centre location (0,0) is at RA = $8^{h}40^{m}39^{s}$, Dec. = $-52^{d}53^{m}18^{s}$. The labels are the same as the IDs in Table 1.

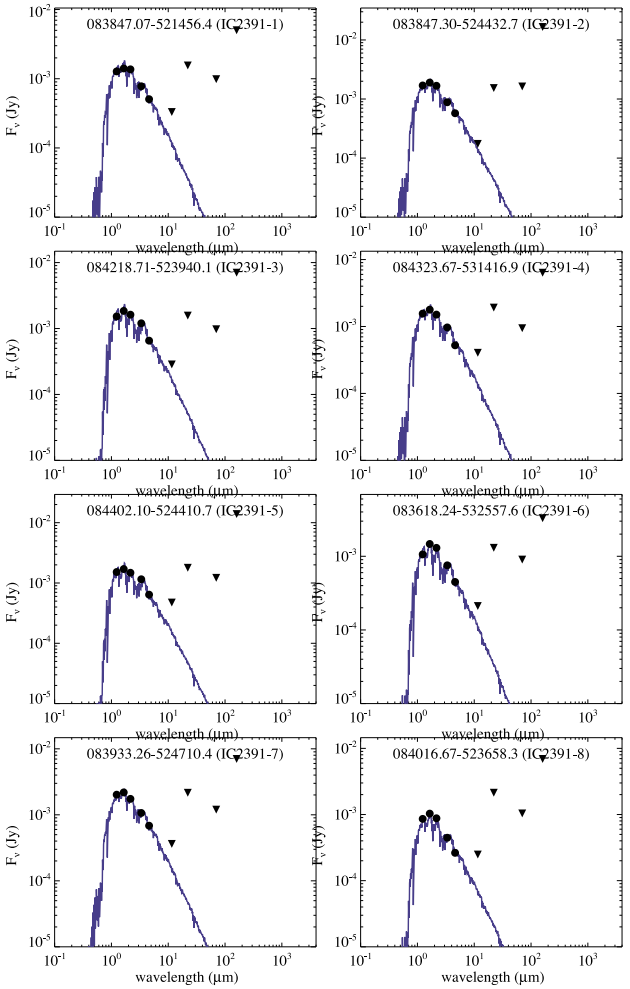

Figure 3. SEDs for the targets. Solid line is the BT Settl model fit to the photosphere. The filled circles and triangles are the observed photometry and upper limits, respectively. The photometry for the target ID #5 was found in the AllWISE Reject Table, because it is affected by a diffraction spike from a nearby star.

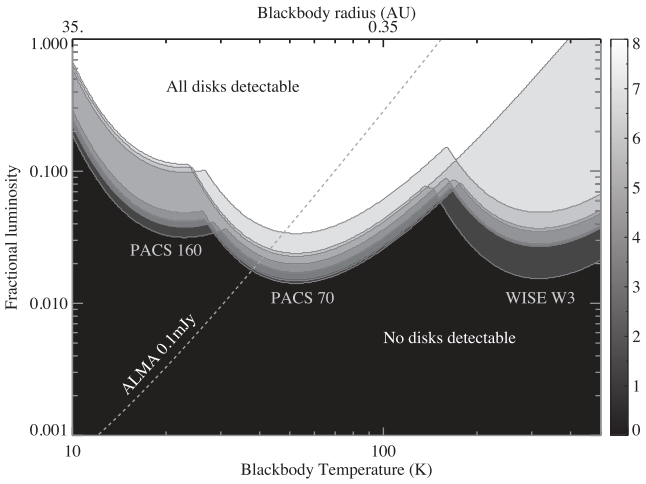

Figure 4. Sensitivity to blackbody emission around survey targets (3σ). The top and bottom axes show the corresponding radius and blackbody temperature, respectively. Each of the eight lines shows the sensitivity for a specific target (IDs marked on the right axis), with different minima corresponding to different instruments of PACS 160 and 70 μm and *WISE* 12 μm (W3) (from left to right). Each contour level shows the number of brown dwarfs around which discs at specific locations in the parameter space could have been detected. Also shown is the expected sensitivity for an ALMA observation with a 3σ noise level of 0.1 mJy.

blackbody emission from a disc at some specific radius, but the limits are otherwise entirely model independent. The bottom axis shows the disc blackbody temperature, and the top axis shows the corresponding radius where the dust material is located, assuming $L_\star = 0.002\,L_\odot$. Each individual curve shows the combined limits for each brown dwarf, with different troughs corresponding to PACS 160 and 70 μm, and the *WISE* 12 μm bands (from left to right, as labelled). The *WISE* 22 μm curves are present, but barely visible since the PACS and *WISE* 12 μm data give better sensitivity at temperatures of around 200 K. Each minimum corresponds to the blackbody peak at one of the observed wavelengths (i.e. PACS 70 μm is most sensitive to 50 K emission), showing that observations at a range of wavelengths are needed to constrain emission at a range of disc radii.

Combining all contours shows how many of the eight observations could have detected a disc at any point in the given parameter space. No discs with fractional luminosities lower than about 1 per cent could have been detected for any target, whereas discs with fractional luminosities greater than about 10 per cent could have been detected for most targets at most disc temperatures. Also plotted is the expected sensitivity for an Atacama Large Millimeter/sub-millimeter Array (ALMA) observation with a 3σ noise level of 0.1mJy, showing that ALMA is sensitive to brown dwarf debris discs with fractional luminosities $\gtrsim$0.1 per cent that lie at a few tens of au.

For low-mass stars with $T_{\rm eff}$ of 3000–5000 K and at ages of ∼10–400 Myr, the observed fractional dust luminosities range between 10^{-5} and 10^{-3} (e.g. Low et al. 2005; Lestrade et al. 2006, 2012; Plavchan et al. 2009). Among these is the well-known M dwarf debris disc system of au Mic (∼12 Myr old), with a fractional luminosity of $\sim 6 \times 10^{-4}$ (Liu et al. 2004). For nearby (within ∼20 pc) FGK-type fields stars (∼0.1–10 Gyr) observed under the *Hershcel* DUst around NEarby Stars survey, the fractional dust luminosities are estimated to be between $\sim 7 \times 10^{-7}$ and 3×10^{-4} (Eiroa et al. 2012). Among the M dwarfs observed by Siegler et al. (2007) in

IC 2391, even the brightest debris disc may just be approaching an ∼1 per cent fractional luminosity, depending strongly on the assumed dust temperature. At younger ages, the ∼10 Myr old M dwarf debris discs TWA 7 and TWA 13AB have fractional luminosities of 10^{-3}–10^{-4} (Low et al. 2005). The faintness of late-type stars means that detecting infrared excesses becomes increasingly difficult, and detections are therefore biased towards the brightest discs (e.g. Plavchan et al. 2009). The PACS observations are therefore not sensitive enough to detect debris discs around IC 2391 brown dwarfs at fractional luminosities similar to those observed among late-type stars, which are at the same or even younger ages.

3.2 Disc fractions versus stellar mass and age

In Fig. 5, we have plotted the disc frequencies at ages of ∼1–100 Myr, for three different mass bins. For the 'young' (∼1–10 Myr) group, we have used the spectral type range of B5–K5 for the bin of high-mass stars (∼1–4 $M_\odot$), the spectral range K7–M5 for low-mass stars (∼0.1–1 $M_\odot$), and spectral type later than M5 for brown dwarfs (<0.08 $M_\odot$). The (rough) thresholds for the bins have been determined using the evolutionary models by Baraffe et al. (2003). For the 'old' age group (>10 Myr), given the discrepancies in the spectral type coverage from the various surveys, it is difficult to use the same spectral type boundaries for all clusters. At ages of ∼30–100 Myr, the ∼1 $M_\odot$ mass boundary would roughly correspond to a K0–K3 spectral type. However, most surveys at these ages have focused on BAFG stars, with a few, if any, KM-type stars included in the sample. To be consistent with previous comparative studies on debris discs, we have used the same spectral type range in a bin for these older clusters as considered by Siegler et al. (2007). In NGC 2547, the high-mass bin consists of B8–A9 stars, while the low-mass bin covers the F0–F9 spectral range. In IC 2391, the high-mass bin has B5–A9 stars, and low-mass covers the F2–K4 range. In Pleiades, the high-mass range is the same as IC 2391, while the low-mass range has F3–K6 stars.

The data points in Fig. 5 circled in black are debris disc fractions, while the rest of the points represent primordial disc fractions. The criteria for distinguishing between primordial and debris discs is described in Carpenter et al. (2009) and Riaz et al. (2012). The primordial discs, as they are defined, are the ones that show excess emission at ≤10 μm wavelengths, which probe the inner regions at radii within ∼1–5 au in these discs. Debris discs are photospheric

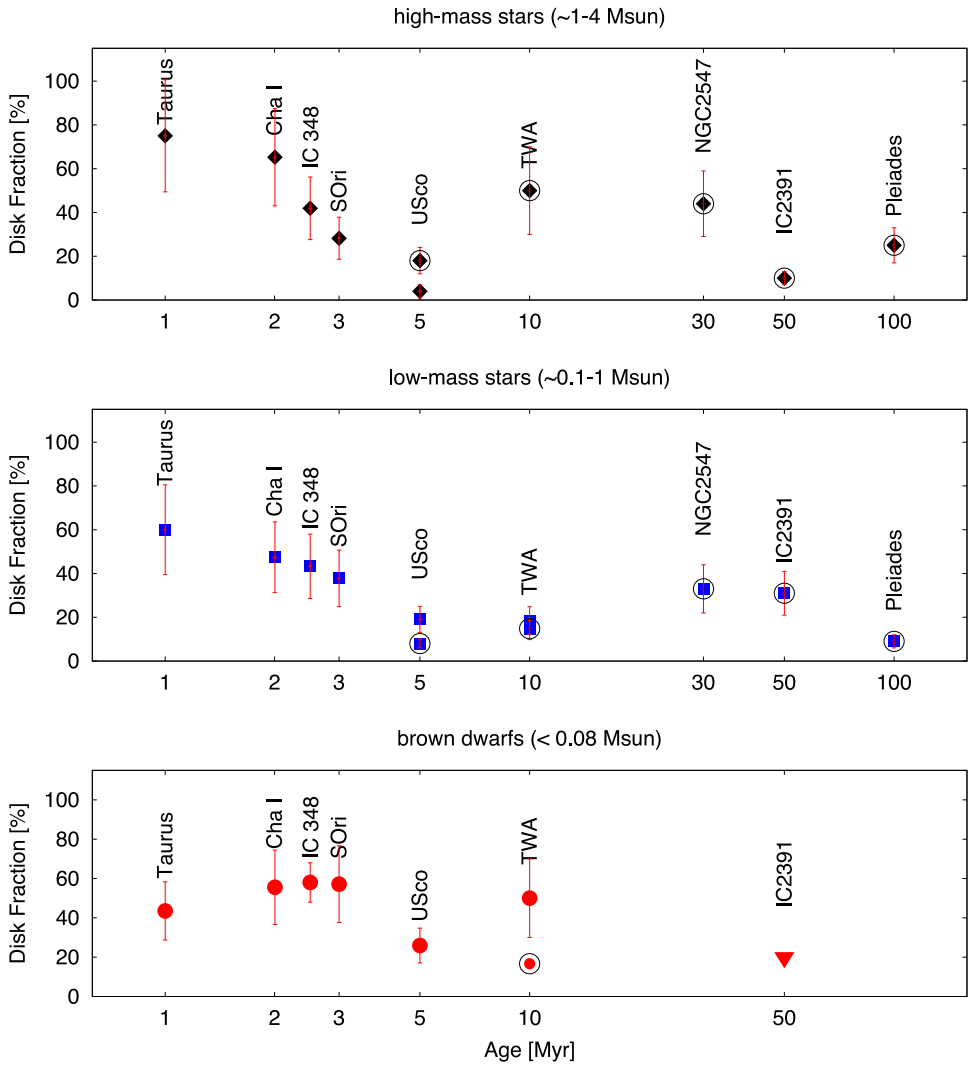

Figure 5. The disc fractions versus stellar age for the high-mass stars (top), low-mass stars (middle) and brown dwarfs (bottom). Debris disc fractions are circled in black. The primordial disc fractions are based on the presence of excess emission at ≤10 μm wavelengths, whereas the debris discs are photospheric at these wavelengths but show excess at 24 and/or 70 μm. For IC 2391 brown dwarfs, the red triangle denotes the upper limit to the primordial disc fraction.

Table 2. Disc fractions.

Name	Disc fraction (per cent)			References
	High-mass	Low-mass	Brown dwarfs	
Taurus[a]	75 ± 26	60 ± 20	43 ± 15	1, 2
Cha I[a]	65 ± 22	47 ± 16	55 ± 19	1, 2
IC 348[a]	42 ± 14	43 ± 15	58 ± 10	1, 2
σ Orionis[a]	28 ± 10	38 ± 13	57 ± 19	1, 2
USco[b]	4 ± 3, 18 ± 6	19 ± 6, 8 ± 2	26 ± 9	3, 4, 5, 6
TWA[c]	50 ± 20	9 ± 3, 18 ± 6	50 ± 20	4, 7, 8
NGC 2547[d]	44 ± 15	33 ± 11	–	9, 10
IC 2391[e]	10 ± 3	31 ± 10	≤30	11, 12
Pleiades[f]	25 ± 8	9 ± 3	–	13, 14

[a]These discs are classified as primordial/evolved discs. The debris disc fraction for the younger clusters is negligible (∼1–2 per cent).
[b]The first value is for primordial discs, second value for debris discs. The brown dwarf discs are all classified as primordial/evolved discs. The total disc fraction for high-mass stars is 22 ± 7 per cent, and for low-mass stars is 27 ± 9 per cent.
[c]For the high-mass stars, all discs are classified as debris sources. For the low-mass stars, the first value is for primordial discs, second value for debris discs. The brown dwarfs are all classified as primordial/evolved discs. The total disc fraction for low-mass stars is 21 ± 7 per cent.
[d]High-mass and low-mass bins cover the spectral ranges of B8–A9 and F0–F9, respectively.
[e]High-mass and low-mass bins cover the spectral ranges of B5–A9 and F2–K4, respectively.
[f]High-mass and low-mass bins cover the spectral ranges of B5–A9 and F3–K6, respectively.
References: (1) Luhman et al. (2008); (2) Luhman et al. (2010); (3) Carpenter et al. (2009); (4) Riaz et al. (2009); (5) Scholz et al. (2007); (6) Riaz et al. (2012); (7) Low et al. (2005); (8) Schneider et al. (2012); (9) Gorlova et al. (2007); (10) Young et al. (2004); (11) Siegler et al. (2007); (12) This work; (13) Gorlova et al. (2006); (14) Stauffer et al. (2005).

at these wavelengths, but show excess emission at 24 μm and/or 70 μm, which arises from the outer disc regions at radii >1–5 au. A compilation of the disc fractions with references is provided in Table 2. We have also compared our Upper Scorpius (USco) fractions with the ones provided for different spectral type bins in Luhman & Mamajek (2012). These bins have slightly different boundaries than the ones we have considered. The criteria used for classifying primordial/debris discs are also different. If we combine the Luhman & Mamajek fractions for their B8–M0 bins, then the primordial fraction (from 8 μm excess) is ∼7 per cent, and the debris disc fraction (from 24 μm excess) is ∼25 per cent. These fractions are higher but still comparable within the uncertainties to the USco fractions for the high-mass bin in Table 2. Likewise, the low-mass and brown dwarf bin fractions for USco in Table 2 are comparable but slightly higher than the M0–M4 and M4–M8 fractions from Luhman & Mamajek (2012). These slight differences in fractions are expected due to the different spectral type bins. We note that a recent analysis by Pecaut et al. (2012) indicates the possibility for the age of USco to be older (∼11 Myr) than the widely considered estimate of ∼5 Myr in various disc studies (e.g. Carpenter et al. 2009; Riaz et al. 2012). Pecaut et al. have argued that an older age would be consistent with a null excess fraction for F-type stars in USco, with the excess frequency determined from Hα and/or *K*-band excess emission. However, these indicators probe the warm inner edge of the disc, and the disc material in the innermost (<0.1 au) region is observed to be dissipated within 2–3 Myr of age (e.g. Haisch et al. 2001). If USco is indeed as old as the TW Hydrae Association (TWA), then we would not expect to see excess emission in the mid-infrared IRAC or *WISE* bands at wavelengths shortwards of ∼10–12 μm, which probe the primordial disc material at radii within ∼1–2 au. For all three categories of stars shown in Fig. 5, an older age for USco would not be consistent with the still existent primordial discs in this association, based on the mid-infrared excess emission. We have therefore placed this point at 5 Myr, following previous disc studies.

By an age of ∼5–10 Myr, the primordial disc fractions for the high-mass and low-mass stars have reached their lowest point; only ∼10–20 per cent of the discs at these ages are in the primordial phase, which indicates that a large number of these discs have experienced significant inner disc clearing (e.g. Carpenter et al. 2009). The disc fractions then show a rise again, from ∼20 per cent at 10 Myr to ∼40 per cent at ∼30 Myr. These older discs are found to be optically thin and gas poor, and have been classified as debris disc systems (e.g. Rieke et al. 2005; Siegler et al. 2007). Thus, by an age of ∼10 Myr, the inner disc material is significantly dissipated for the high- and low-mass stars, and the discs have made a clear transition to the debris phase. The rise in the debris disc fraction for the high-mass stars between ∼50 and 100 Myr could be a sample size difference, since the Pleiades sample studied by Gorlova et al. (2006) is about twice the BA-type star sample studied by Siegler et al. (2007) in IC 2391.

The bottom panel in Fig. 5 shows the disc fractions for brown dwarfs, which are based on ∼3–24 μm observations, and probe radii <1 au in these discs. No clear age dependence is evident in the case of the sub-stellar sources, as the primordial disc fraction appears to be nearly constant between 1 and 10 Myr, except a dip at 5 Myr, which is likely due to a different formation mechanism for USco brown dwarfs and/or the higher brown dwarf to star number ratio in

this particular association, as argued in Riaz et al. (2012). The general picture thus indicates that protoplanetary discs around brown dwarfs tend to remain in the primordial stage for a relatively longer time-scale compared to higher mass stars (e.g. Riaz & Gizis 2008). As mentioned, none of the eight IC 2391 targets were detected in the *WISE* 12 and 22 μm bands. The *WISE* 5σ point source sensitivity at 12 and 22 μm is ∼0.7 and ∼5 mJy, respectively (*WISE* Explanatory Supplement). The predicted photospheric fluxes at these wavelengths for an M6 dwarf are ∼0.1–0.2 mJy. Thus, while it is impossible to detect the photospheres at these wavelengths, the IC 2391 brown dwarfs may possess weak mid-infrared excesses, with an observed to photospheric flux ratio $F_{\rm obs}/F_{\rm phot}$ of <3. In comparison, the primordial brown dwarf discs in the ∼10 Myr old TWA exhibit large 12 μm excesses, with $F_{\rm obs}/F_{\rm phot} > 8$–10 (Riaz et al. 2012). The non-detections for the IC 2391 cases then suggests that there has been significant inner disc clearing, and that the discs around brown dwarfs have transitioned to the debris phase by ∼40–50 Myr ages, resulting in photospheric emission and/or negligible excesses at mid-infrared wavelengths.

A similar argument can be applied for the PACS wavebands. If we compare the PACS 70 μm upper limits for the IC 2391 targets with the observed flux densities in this band for the primordial 1–10 Myr brown dwarf discs (Harvey et al. 2012; Riaz & Gizis 2012), then nearly 80 per cent of these discs lie above the 2σ upper limit, while the rest have fluxes at the 1σ limit. Thus, there is a strong likelihood that any primordial discs with similar brightness and fractional luminosities as observed for the younger brown dwarfs would be within our survey detection limits and could have been detected. We can test this by applying a simple exact binomial test using the null hypothesis that there is an equal probability of detecting or not detecting a primordial disc in a single observation. The one-tailed probability of detecting a primordial disc for six out of eight IC 2391 targets is quite high, about 96 per cent. The *P*-value of 0.96 is significantly strong, being nearly a factor of 20 higher than the significance level of 0.05, thus making the null hypothesis valid. The null detection rate despite such a high probability again indicates that a majority of the brown dwarf discs have transitioned to the debris stage by this age. Given that there is presumably a range of primordial disc brightnesses, the fraction of primordial brown dwarf discs for IC 2391 cannot be definitively set to 0 per cent, but can perhaps be set to <20 per cent (Fig. 5), in comparison with the detection likelihood of the younger disc sources. We note that a large number of primordial brown dwarf discs have not been observed yet at PACS wavelengths, and so the fraction that lies above our detection limits could be smaller than ∼80 per cent. Nevertheless, our PACS survey has helped set limits on the primordial disc lifetime to be <40 Myr for the sub-stellar sources.

The PACS observations, unfortunately, do not provide any constraints on the debris disc evolution around brown dwarfs. The conclusion from Fig. 4 was that typical debris discs with fractional luminosities similar to those observed for low-mass stars could *not* have been detected given the sensitivities of our survey. In other words, Vega-like debris discs at $L_{\rm D}/L_{*} \leq 10^{-3}$ levels could exist around the IC 2391 brown dwarfs, and the fraction could be as high as ∼30 per cent, as observed for low-mass stars at these ages (e.g. Siegler et al. 2007). It is worth noting that there is one candidate brown dwarf debris disc in the TWA (2MASS J1139511−315921), which shows a small excess at 24 μm with $F_{\rm obs}/F_{\rm phot} \sim 3$, indicating the presence of warm dust around it. This object was undetected in the follow-up PACS 70 μm observations, and it was argued that the debris disc has a very low fractional luminosity of $L_{\rm D}/L_{*} \sim 10^{-5}$, thus lying below the detection limit (Riaz & Gizis 2012).

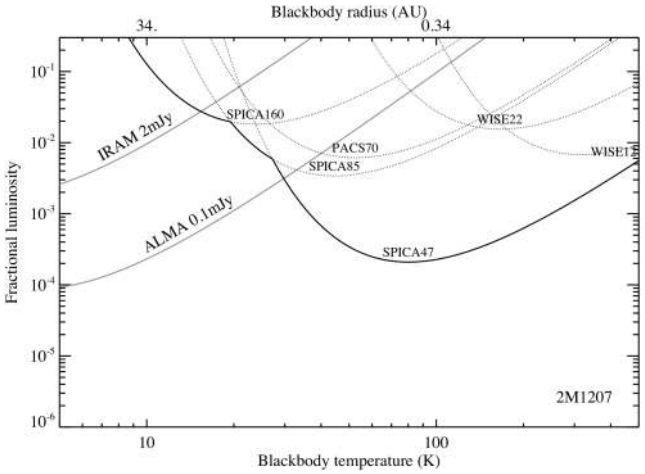

Figure 6. A sensitivity plot for the ∼10 Myr old 2M1207 brown dwarf disc in the TWA. Axes represent the same parameters as shown in Fig. 4. Further details are provided in the text.

The presence of this candidate suggests a transition to the debris phase for brown dwarfs may have begun at ∼10 Myr, and perhaps all sub-stellar debris systems are at such low fractional luminosities of $\sim 10^{-5}$. The debris disc fraction might increase thereafter between 10 and 40 Myr, or it might rapidly decline during this short time-scale. A rapid debris dispersal would be consistent with the trends noted by e.g. Gorlova et al. (2007) and Plavchan et al. (2009) for M-type debris systems, and by e.g. Siegler et al. (2007) for the FGK debris discs, which appear to decay over a comparatively faster time-scale than BA-type stars, although these trends are not definitively confirmed, and the samples studied for M-type stars are much smaller in size compared to the earlier type sources.

Future observations particularly with the SpicA FAR-infrared Instrument imager onboard the *SPICA* space observatory, will be ideal to complete the census of brown dwarf discs, both in the primordial and debris phases. As an example, in Fig. 6, we have plotted the sensitivities similar to Fig. 4 for the case of the ∼10 Myr old brown dwarf disc 2MASSW J1207334−393254 (2M1207) in the TWA, located at a distance of ∼50 pc (Mamajek 2005). This is presently the oldest known brown dwarf disc which has been detected in the far-infrared. The *WISE* and PACS limits are from actual observations (Harvey et al. 2012). The *SPICA* sensitivities have been calculated using the confusion limits of 0.015, 0.5 and 5 mJy in the SW (34–60 μm), MW (60–110 μm) and LW (110–210 μm) bands. The IRAM 30m telescope (IRAM) and ALMA limits are as marked. The main conclusion that can be made from this figure is that for probing dust temperatures of a few tens to a few hundreds of Kelvins at distances of within 1 au or the habitable zone from a central brown dwarf, the *SPICA* SW band would be the most suitable one, simply because the confusion limit is much fainter. ALMA is better at cooler temperatures. The IRAM/NIKA 1.2 mm band, however, would be sensitive to brighter discs of >1 per cent fractional luminosity, similar to the sensitivity of our present PACS survey. We also note that the 2M1207 disc was undetected in the SPIRE ∼200–500 μm observations, which were sensitive to ∼2 mJy level (Riaz & Gizis 2012). Therefore, high-quality observations of large-sized samples with *SPICA* and ALMA in the far-infrared/sub-millimetre domain should provide clues to the dispersal processes and time-scales for discs around sub-stellar objects.

4 SUMMARY

We have conducted a search for discs around brown dwarfs in the ∼40–50 Myr cluster IC 2391. None of the eight targets were detected in any of the PACS bands. We estimate our survey to be sensitive to fractional debris disc luminosities of >1 per cent, and therefore only the brightest debris disc systems, if they existed, could have been detected. We suggest that debris discs of similar levels ($L_D/L_* \leq 10^{-3}$) as those observed around low-mass stars at ∼40–50 Myr ages could exist around the IC 2391 targeted brown dwarfs, but be missed by our survey. It may also be the case that disc dispersal processes such as grain growth and terrestrial planet formation occur at a faster rate around brown dwarfs, once they have entered the secondary debris phase, resulting in a non-detection at later ages. Most primordial discs with flux densities similar to those observed among younger ∼1–10 Myr brown dwarfs would be within our survey detection limits and could have been detected. The upper limits from our PACS survey can thus set a constraint of <40 Myr on the primordial disc lifetime for brown dwarfs.

ACKNOWLEDGEMENTS

This work was supported by the European Union through ERC grant number 279973 (GMK). *Herschel* is an ESA space observatory with science instruments provided by European-led Principal Investigator consortia and with important participation from NASA. This publication makes use of data products from the *Wide-field Infrared Survey Explorer*, which is a joint project of the University of California, Los Angeles and the Jet Propulsion Laboratory/California Institute of Technology, funded by the National Aeronautics and Space Administration.

REFERENCES

Allard N. F., Allard F., Hauschildt P. H., Kielkopf J. F., Machin L., 2003, A&A, 411, 473
Baraffe I., Chabrier G., Barman T. S., Allard F., Hauschildt P. H., 2003, A&A, 402, 701
Barrado y Navacués D., Stauffer J. R., Jayawardhana R., 2004, ApJ, 614, 386
Beichman C. A. et al., 2006, ApJ, 652, 1674
Boudreault S., Bailer-Jones C. A. L., 2009, ApJ, 706, 1484
Burns J. A., Lamy P. L., Soter S., 1979, Icarus, 30, 1B
Calvet N., Briceo C., Hernndez J., Hoyer S., Hartmann L., Sicilia-Aguilar A., Megeath S. T., D'Alessio P., 2005, AJ, 129, 935
Carpenter J. M., Mamajek E. E., Hillenbrand L. A., Meyer M. R., 2009, ApJ, 705, 1646
Chen C. H., Jura M., Gordon K. D., Blaylock M., 2005, ApJ, 623, 493
Dullemond C. P., Dominik C., 2004, A&A, 417, 159
Eiroa C. et al., 2013, A&A, 555, A11
Gorlova N., Rieke G. H., Muzerolle J., Stauffer J. R., Siegler N., Young E. T., Stansberry J. H., 2006, ApJ, 649, 1028
Gorlova N., Balog Z., Rieke G. H., Muzerolle J., Su K. Y. L., Ivanov V. D., Young E. T., 2007, ApJ, 670, 516
Gullbring E., Hartmann L., Briceño C., Calvet N., 1998, ApJ, 492, 323
Haisch K. E., Jr, Lada E. A., Lada C. J., 2001, ApJ, 553, L153
Harvey P. M. et al., 2012, ApJ, 755, 67
Hillenbrand L. A., 2008, Phys. Scr. T, 130, 014024
Kennedy G. M., Wyatt M. C., Kalas P., Duchêne G., Sibthorpe B., Lestrade J.-F., Matthews B. C., Greaves J., 2014, MNRAS, 438, L96
Lestrade J.-F., Wyatt M. C., Bertoldi F., Dent W. R. F., Menten K. M., 2006, A&A, 460, 733
Lestrade J.-F. et al., 2012, A&A, 548, A86
Liu M. C., Matthews B. C., Williams J. P., Kalas P. G., 2004, ApJ, 608, 526
Low F. J., Smith P. S., Werner M., Chen C., Krause V., Jura M., Hines D. C., 2005, ApJ, 631, 1170
Luhman K. L., Mamajek E. E., 2012, ApJ, 758, 31
Luhman K. L., Hernández J., Downes J. J., Hartmann L., Briceño C., 2008, ApJ, 688, 362
Luhman K. L., Allen P. R., Espaillat C., Hartmann L., Calvet N., 2010, ApJS, 186, 111
Mamajek E., 2005, ApJ, 634, 1385
Miville-Deschenes M.-A., Lagache G., ApJS, 157, 302
Muzerolle J., Calvet N., Hartmann L., 1998, ApJ, 492, 743
Pecaut M. J., Mamajek E. E., Bubar E. J., 2012, ApJ, 746, 154
Pilbratt G. L. et al., 2010, A&A, 518, 1
Platais I. et al., 2007, A&A, 461, 509
Plavchan P., Werner M. W., Chen C. H., Stapelfeldt K. R., Su K. Y. L., Stauffer J. R., Song I., 2009, ApJ, 698, 1068
Poglitsch A. et al., 2010, A&A, 518, 2
Quillen A. C., Blackman E. G., Frank A., Varnière Peggy, 2004, ApJ, 612, L137
Riaz B., Gizis J. E., 2008, ApJ, 681, 1584
Riaz B., Gizis J. E., 2012, A&A, 548, 54
Riaz B., Lodieu N., Gizis J. E., 2009, ApJ, 705, 1173
Riaz B., Lodieu N., Goodwin S., Stamatellos D., Thompson M., 2012, MNRAS, 420, 2497
Rice W. K. M., Wood K., Armitage P. J., Whitney B. A., Bjorkman J. E., 2003, MNRAS, 342, 79
Rieke G. H. et al., 2005, ApJ, 620, 1010
Schneider A., Song I., Melis C., Zuckerman B., Bessell M., 2012, ApJ, 757, 163
Scholz A., Jayawardhana R., Wood K., Meeus G., Stelzer B., Walker C., O'Sullivan Mark, 2007, ApJ, 660, 1517
Setiawan J., Henning Th., Launhardt R., Müller A., Weise P., Kürster M., 2008, Nature, 451, 38
Siegler N., Muzerolle J., Young E. T., Rieke G. H., Mamajek E. E., Trilling D. E., Gorlova, Nadya; Su, Kate Y. L., 2007, ApJ, 654, 580
Spezzi L. et al., 2009, A&A, 499, 541
Srom K. M., Strom S. E., Edwards S., Cabrit S., Skrutskie M. F., 1989, AJ, 97, 1451
Stauffer J. R. et al., 2005, AJ, 130, 1834
Su K. Y. L. et al., 2006, ApJ, 653, 675
Trilling D. E. et al., 2008, ApJ, 674, 1086
van Leeuwen F., 2007, A&A, 474, 653
Wright E. L. et al., 2010, AJ, 140, 1868
Wyatt M. C., 2008, ARA&A, 46, 339
Young E. T. et al., 2004, ApJS, 154, 428

This paper has been typeset from a TEX/LATEX file prepared by the author.